# A MULTI-FREQUENCY STUDY OF EXTRAGALACTIC JETS

**A. C. Sadun, P. B. Rimmer**
University of Colorado at Denver
Campus Box 157, P.O. Box 173364, Denver, CO 80217-3364
ASADUN@CARBON.CUDENVER.EDU, PBRIMMER@OURAY.CUDENVER.EDU

## Abstract

We intend to go through the Very Large Array, *Hubble* Space Telescope, and *Chandra* X-ray Observatory databases, among others, to scrutinize more closely observations made of extragalactic jets. Accordingly, we have constructed our own database of extragalactic jets, those that have been observed in the radio and either optical or X-ray wavebands. The purpose of studying jets at widely spaced frequencies with this database as an analytic tool is several-fold. First, by developing correlations among various emission characteristics, one can further delineate the FRI/FRII dichotomy. Indeed, we have already found that there is a strong correlation between the inverse Compton process and FRII jets. Secondly, we can use this database to identify X-ray and optical candidates for further study with *HST*, and *Chandra*. Thirdly, we can identify and further process archival data from the VLA, *HST*, and *Chandra* databases for many of these objects. We did just this with an *HST* archival image of 4C30.31, with the result of uncovering a heretofore unknown double optical jet corresponding to the radio jets already well known. Finally, we can identify optical candidates for searches with ground-based telescopes, to look for counterparts to radio and X-ray jets. Again, as proof of concept, we did this for three sources, the result being that one and possibly a second show some optical extension corresponding to a jet. Therefore, the use of such high resolution databases is critical in furthering the understanding of extragalactic jets, and is of invaluable assistance in performing this study.

## 1 Introduction

This is a horizontal study of extragalactic kpc-scale jets, particularly of their morphologies and broad band spectra. It is only recently that we have the opportunity to investigate the radiation mechanisms carefully for many such jets. We are now in the position to exploit new technologies, principally the *Hubble* Space Telescope (*HST*) and the *Chandra* X-ray Observatory (*Chandra*), and be able to explain the dynamics of many jets over ten decades of frequency if one includes radio data. To do this, we need both high sensitivity as well as high resolution; we have had this capability in the radio, through the Very Large Array (VLA) and other synthetic aperture radio telescope arrays, for a few decades now. However, it has only been with the advent of *HST* in the optical, and most recently with *Chandra* in X-ray that we have been able to have similar capabilities at higher frequencies, extending to a much greater spectral range. This is important because while jets in the radio are almost exclusively due to the synchrotron mechanism, this cannot be said necessarily in the optical or X-ray. In many cases, it can be shown that higher energy radiation is due to Compton scattering off the synchrotron radio photons (SSC), or off the optical or infrared (IR) radiation of the active galactic nucleus (AGN) itself, or off the cosmic microwave background (CMB) radiation. Likewise, the higher energy radiation could still be due to synchrotron radiation alone. By analyzing the spectrum over a minimum of two and preferably three wavelength regimes, one should be able to get a much more precise determination of the overall dynamics of the jet in question. A comparison of morphologies at different wavelengths also gives us clues to the dynamics of the system in question.

This study in relativistic astrophysics leads us to learn more about galaxy and AGN evolution, help us categorize extragalactic jets and elucidate better the FRI/FRII dichotomy, and even allow us to use such new-found knowledge of jets as a probe to the central engine of the AGN itself, as well, on the distal end, as a probe into the intergalactic medium. We begin by doing a thorough literature search and establishing a database

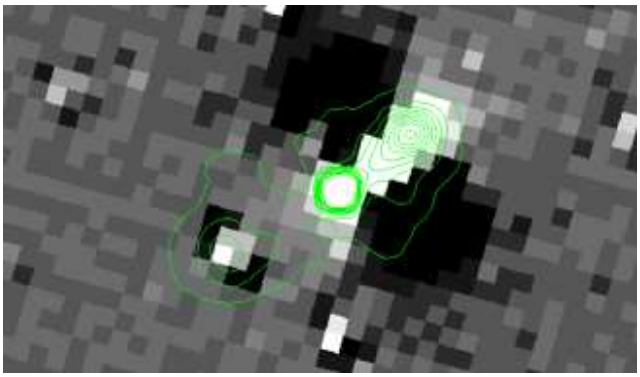

Figure 1: Grey-scale image of 4C30.31 taken by *HST* in R (after galaxy subtraction), with VLA overlay (linear contours). North is up and East is left. End to end separation of the lobes is around $2'$ (685 kpc).

of radio jets having higher frequency data that could be exploited for further observation and analysis (see Table 4 to Table 7). Unspecified observations are designated with an X. S designates synchrotron, IC inverse Compton, and C *Chandra*. Energy spectral index $\alpha$ is shown for several wavelengths where available.

## 2 Statistics and Correlations

The database can be analyzed in the aggregate in terms of finding statistics of and correlations among the various jets. Some of the statistics that we would compile include the number of jets observed in X-ray (with *Chandra*), in optical (with *HST*), the spectral indices at the three main wavelength regimes, radio, optical, and X-ray, the relative number of FRI versus FRII sources, and the corresponding emission mechanisms inferred. We could also investigate the power of jets in the relative wavelength regimes, their length, spectral indices, and what fraction are single jets. The information to yield such statistics is gleaned from both published results as well as further scrutiny of the *HST* and *Chandra* databases. Among the correlations, perhaps the most important ones to consider are how the FR type correlates to emission mechanism (which includes information on spectral indices and power). Also, since the inverse Compton process off the CMB should be independent of redshift (Schwartz, 2002), a correlation of redshift to emission mechanism would be important here as well.

## 3 Database subsets

In looking over our database, we can make a number of lists that would be useful for further study. One list can be of ideal candidates for *Chandra* or even *XMM-Newton* observations. This is obtained by studying particular candidates and results from observations with *HST*. See Table 1.

The same can be done for optical candidates for observation with either *HST*, or in some cases, with ground-based telescopes. We have colleagues who are willing to coordinate their efforts in observing suspected optical jets with ground-based telescopes readily available to them. Again, this information is obtained by looking at the archival data with *HST* and with *Chandra*. See Table 2.

If one were to look for optical jets merely by randomly picking radio jets to observe, the fraction that would reveal anything in the optical would be very small. However, when using the criterion of there being some kind of X-ray signature of a jet, then the chances of success grow dramatically. Indeed, to test this out, we used this criterion to pick three candidates to observe with ground-based optical telescopes. One object, B2 0738+313, showed an optical jet emission that was cospatial and of similar morphology to the X-ray jet observed with *Chandra*. See Fig. 2. A second object, 3C219, showed no optical emission whatsoever, and a third object, 3C9, was ambiguous, and will require longer integration time. Clearly, this encourages us to believe that the aforementioned strategy is a successful one for discovering more optical jets as counterparts to radio and X-ray extragalactic jets. We have colleagues who are willing to assist us in observing particularly exciting candidates in hopes of discovering optical jet counterparts.

The radio morphology of B2 0738+313 looks quite different than in X-ray and optical, perhaps separating regions of synchrotron emission alone with inverse Compton emission. In fact, the possibility exists that the jet has bent enough so that only the proximal portion has detectable inverse Compton emission, while the distal end exhibits radio emission only. Obviously, once an optical counterpart in this kind of exercise is discovered, spectral and morphological analysis as well as inferring the emission mechanism quickly follow. There are also certain jet sources, that when scrutinized carefully from the archives, lend themselves well to particularly detailed or unusual theo-

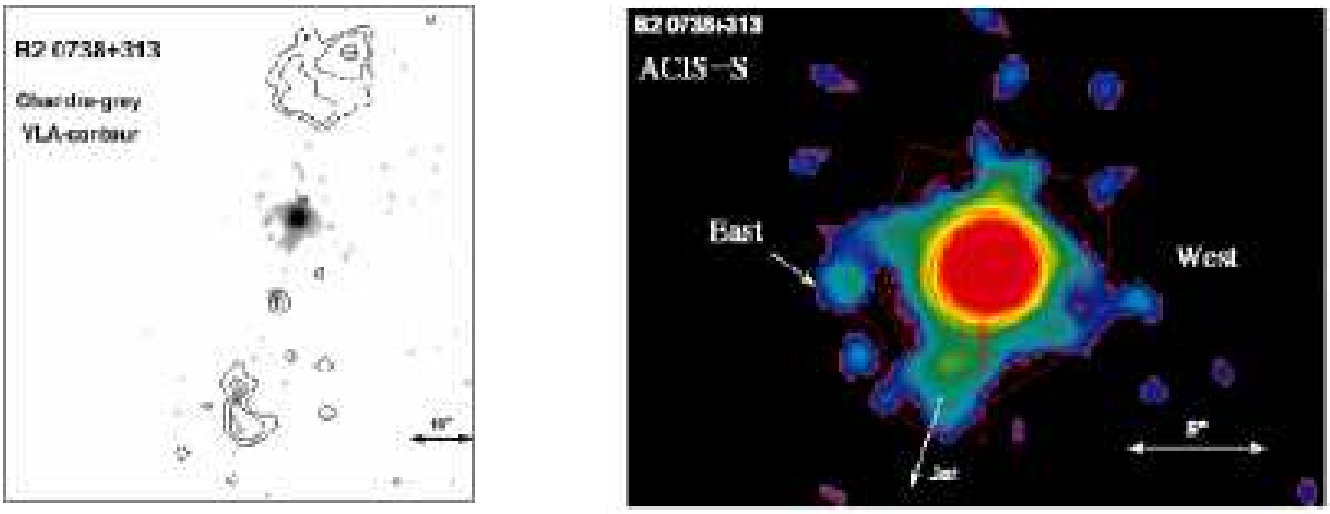


Figure 2: (a) Superposition of *Chandra* X-ray image (gray scale) with optical contours. (b) Superposition of B2 0738+313 *Chandra* X-ray image (gray) with the VLA high-resolution radio (1.4 GHz contours) (Siemiginowska et al., 2003).

retical modeling. This would include not only well-observed jets in several wavelength regimes, but also jets with unusual morphologies indicating jet-cloud interactions. For instance we have done this for the unusual radio jet of Her A (3C348). We developed a phenomenological model to explain the jet seen with rings in radio but not in optical, but whose optical image reveals a double nucleus in the underlying galaxy itself (Mason & Morrison, 1988; Meier & Sadun, 1991; Sadun & Hayes, 1993; Morrison & Sadun, 1996; Sadun & Morrison, 2002). Finally, there are a number of radio jets that can be located within an elliptical galaxy, so that in the optical, the jet would be obscured by the galactic component. Through the judicious use of model galaxy subtraction and other image processing techniques, the optical jet can often be teased out of the image. As a test, this was done with an *HST* image of 4C30.31 (B2 1658+30A) to very good effect. We uncovered a clear double jet in the optical co-spatial with the radio jets, where a double optical jet had never been seen before (Fig. 1). We feel that there are many such opportunities, by scouring the *HST* archive, to uncover other jets in the optical, through careful use of image processing techniques. Sophisticated image processing could also be brought to bear in X-ray images through the *Chandra* archives as well.

## 4 Theoretical considerations

The emission mechanism responsible for optical jets may be pure synchrotron, or Compton scattering off of a variety of photon sources (synchrotron radio photons, cosmic microwave background, radiation from the core AGN radio or IR emission, or a jet-cloud collision or interaction of some sort). Due to the relatively short lifetimes of synchrotron photons in the visible, and the large scale of the extragalactic jets, many believe that there must be re-acceleration, and thus, re-acceleration is not altogether necessary, although certainly possible (Sharpa & Urry, 2002). Therefore optical knots along the jet are sites of such re-acceleration.

If the emission mechanism is Compton scattering, the angle to the line of sight is expected to be smaller, although the Lorentz factor $\Gamma$ of the relativistic electrons in question is also expected to be smaller than for pure synchrotron. It would be quite interesting to see what proportion of optical jets could be explained by synchrotron emission alone, and which proportion show a spectrum that indicates the presence of Compton scattering. Indeed, there are a number of sources that show hot spots in the optical or even X-ray. (See Table 3). These are typically due to inverse Compton emission, and are FRII sources.

This supports the important observation that within the jets of the database, there is a strong correlation between those jets which show the presence of inverse Compton emission and those sources designated as FRII sources. Indeed, perhaps this is to be expected, as inverse Compton emission requires bulk relativistic motions far from the core, and by definition only FRII jets show such motions on such scales, whereas FRI sources flare and decelerate (Jester, 2003).

## 5 Conclusion

With the advent of the *HST* and now, more recently, of other superb imaging technologies in X-ray, particularly *Chandra*, we have the opportunity to study large numbers of extragalactic jets over a broad range of frequencies. We can study their emission mechanisms as well as their differing morphologies. Over the years, we have developed good criteria to distinguish two classes of AGN and their jets with the Fanaroff-Riley designation. The tools and data are now available to refine further those classes, and to discover better what physical processes they represent. However, this can only be pursued through the thorough and judicious use of archival imaging data, particularly that of the VLA, *HST* and *Chandra*, although others would contribute as well.

## References

Jester, S. 2003, private communication
Mason, A., Morrison, P. 1988, *Nature*, 333, 640
Meier, D,. Sadun, A. 1991, ApJ, 379, 141
Morrison, P., Sadun, A. 1996, MNRAS, 278, 265
Sadun, A., Hayes, J. J. E. 1993, PASP, 105, 379
Sadun, A., Morrison, P. 2002, AJ, 123, 2312
Schwartz, D. A. 2003, ApJ, 569, L23
Sharpa, R., Urry, C. M. 2002, New Astron. Rev., 46, 405
Siemiginowska, A., et al. 2003, ApJ, 569, 643

Table 1: *HST* candidates

| Object | z | Emission | l (kpc) | L (arcsec) | FR | a(r) | a(r-o) | a(o-x) | a(x) |
|---|---|---|---|---|---|---|---|---|---|
| B2 0206+35 | 0.037 | S | 2 | 2 | I | | | | 1.05 |
| B2 0326+39 | | | | | I | | | | |
| PKS 0606−085 | 0.872 | | | | | | | | |
| B2 0738+313 | 0.630 | IC/CMB | 200 | 35 | II | 0.9 | | | 1.01 |
| B2 0827+243 | 0.941 | | | | | | | | |
| PKS 0920−397 | 0.591 | | | | | | | | |
| PKS 1030−357 | 1.455 | | | | | | | | |
| PKS 1055+201 | 1.110 | | | | | | | | |
| PKS 1202−262 | 1.950 | | | | | | | | |
| SDSS 1306+0356 | 5.990 | IC/CMB | 158 | 23 | II | | | 1.65 | |
| PKS 1421−490 | | | | | | | | | |
| PKS 1510−089 | 0.361 | | | | | | | | |
| PKS 2101−490 | | | | | | | | | |
| 3C9 | 2.012 | IC/CMB | 57 | 10 | II | 1 | | | 0.6 |
| 3C78 | 0.029 | S | 4 | 5 | I | 0.43 | | | |
| 3C98 | 0.031 | | | | | | | | |
| 3C99 | 0.426 | Collision | 3.7 | 1 | II | 0.82 | | | |
| 3C120 | 0.033 | S | 22 | 25 | I | 0.65 | 0.8 | | |
| 3C129 | 0.021 | S | 1.5 | 2.5 | I | 0.8 | | 0.9 | 0.9 |
| 3C207 | 0.684 | IC/CMB | 48 | 6 | II | 0.9 | | | 0.4 |
| 3C219 | 0.174 | IC/IR | 80 | 40 | II | 0.65 | | | 0.74 |
| 3C223 | 0.137 | | 187 | 120 | II | | | | |
| 3C277.2 | 0.766 | IC/(CMB+Q) | 154 | 20 | II | 0.95 | | | 0.95 |
| 3C284 | 0.239 | | 480 | 174 | II | | | | |
| 3C292 | 0.710 | IC/CMB | 261 | 36 | II | | | | 0.88 |
| 3C303 | 0.141 | SSC+IC/(CMB) | 36 | 17 | II | | | | 1 |
| 3C322 | 1.680 | SSC+IC/(CMB) | 103 | 15 | II | | | | 0.6 |
| 3C334 | 0.555 | | 112 | 16 | II | | | | |
| 4C41.17 | 3.800 | IC/Q | 100 | 15 | II | | | | 0.57 |
| ESO 295−IG022 | 0.055 | IGM interaction | 96 | 90 | | | | | |
| Cen B | 0.012 | IC/CMB | 14 | 472 | I | 0.78 | | | 0.88 |
| Cyg A | 0.056 | SSC | 76 | 62 | I | 0.55 | 1.02 | | 0.8 |
| Fornax A | 0.006 | IC/CMB | 96 | 900 | II | | | | |
| NGC315 | 0.016 | | 64 | 240 | I | | | | |

Table 2: *Chandra* candidates

| Object | z | Emission | l (kpc) | L (arcsec) | FR | a(r) | a(r-o) | a(o-x) | a(x) |
|---|---|---|---|---|---|---|---|---|---|
| B2 0206+35 | 0.037 | S | 2 | 2 | I | | | | 1.05 |
| B2 0326+39 | | | | | I | | | | |
| PKS 0606−085 | 0.872 | | | | | | | | |
| B2 0738+313 | 0.630 | IC/CMB | 200 | 35 | II | 0.9 | | | 1.01 |
| B2 0827+243 | 0.941 | | | | | | | | |
| PKS 0920−397 | 0.591 | | | | | | | | |
| PKS 1030−357 | 1.455 | | | | | | | | |
| PKS 1055+201 | 1.110 | | | | | | | | |
| PKS 1202−262 | 1.950 | | | | | | | | |
| SDSS 1306+0356 | 5.990 | IC/CMB | 158 | 23 | II | | | 1.65 | |
| PKS 1421−490 | | | | | | | | | |
| PKS 1510−089 | 0.361 | | | | | | | | |
| PKS 2101−490 | | | | | | | | | |
| 3C9 | 2.012 | IC/CMB | 57 | 10 | II | 1 | | | 0.6 |
| 3C78 | 0.029 | S | 4 | 5 | I | 0.43 | | | |
| 3C98 | 0.031 | | | | | | | | |
| 3C99 | 0.426 | Collision | 3.7 | 1 | II | 0.82 | | | |
| 3C120 | 0.033 | S | 22 | 25 | I | 0.65 | 0.8 | | |
| 3C129 | 0.021 | S | 1.5 | 2.5 | I | 0.8 | | 0.9 | 0.9 |
| 3C207 | 0.684 | IC/CMB | 48 | 6 | II | 0.9 | | | 0.4 |
| 3C219 | 0.174 | IC/IR | 80 | 40 | II | 0.65 | | | 0.74 |
| 3C223 | 0.137 | | 187 | 120 | II | | | | |
| 3C277.2 | 0.766 | IC/(CMB+Q) | 154 | 20 | II | 0.95 | | | 0.95 |
| 3C284 | 0.239 | | 480 | 174 | II | | | | |
| 3C292 | 0.710 | IC/CMB | 261 | 36 | II | | | | 0.88 |
| 3C303 | 0.141 | SSC+IC/(CMB) | 36 | 17 | II | | | | 1 |
| 3C322 | 1.680 | SSC+IC/(CMB) | 103 | 15 | II | | | | 0.6 |
| 3C334 | 0.555 | | 112 | 16 | II | | | | |
| 4C41.17 | 3.800 | IC/Q | 100 | 15 | II | | | | 0.57 |
| ESO 295−IG022 | 0.055 | IGM interaction | 96 | 90 | | | | | |
| Cen B | 0.012 | IC/CMB | 14 | 472 | I | 0.78 | | | 0.88 |
| Cyg A | 0.056 | SSC | 76 | 62 | I | 0.55 | 1.02 | | 0.8 |
| Fornax A | 0.006 | IC/CMB | 96 | 900 | II | | | | |
| NGC315 | 0.016 | | 64 | 240 | I | | | | |

Table 3: Quasar jet hotspots

| Object | Radio | Optical | X-Ray | z | Emission | l (kpc) | L(arcsec) | FR |
|---|---|---|---|---|---|---|---|---|
| 3C33 | VLA | X | | 0.06 | | | | II |
| 3C65 | VLA | IR | | 1.176 | | | | II |
| 3C111 | VLA | X | | 0.049 | | | | II |
| 3C123 | VLA | IR | *Chandra* | 0.2177 | | | | II |
| 3C184 | VLA | *HST* | *XMM* | 0.996 | | | | II |
| 3C196 | VLA | *HST* | | | | | | II |
| 4C73.08 | X | X | *ROSAT* | 0.0581 | | | | |
| 3C213.1 | VLA | *HST* | | | | | | |
| 3C263 | VLA | *HST* | *Chandra* | 0.656 | SSC | | | II |
| 3C280 | VLA | *HST* | *Chandra* | 0.996 | | | | |
| 3C330 | VLA | *HST* | *Chandra* | 0.549 | SSC | | | II |
| 3C351 | VLA | *HST* | *Chandra* | 0.371 | | | | II |
| 3C354 | X | *HST* | *Chandra* | 0.734 | | | | |
| 3C380 | VLA | *HST* | | | | | | |
| 3C427.1 | VLA | X | X | 0.571 | | | | |
| 3C452 | VLA | X | *Chandra* | 0.0811 | IC/CMB | | | II |

Table 4: Quasar jets

| Object | Radio | Optical | X-ray | z | Emission | l (kpc) | L (arcsec) | FR |
|---|---|---|---|---|---|---|---|---|
| NGC315 | X | *HST* | *Chandra* | 0.0165 | S | 4 | 13 | I |
| B2 0206+35 | VLA | | *Chandra* | 0.0369 | S | 2 | 2 | I |
| B2 0326+39 | | X | *ROSAT* | | | | | I |
| PKS 0521−365 | VLA | *HST* | *Chandra* | 0.05534 | S | 7 | 6.5 | I |
| PKS 0606−085 | X | | *Chandra* | 0.872 | | | | |
| PKS 0637−752 | ATCA | *HST* | *Chandra* | 0.651 | IC/CMB | 100 | 11.5 | II |
| B2 0738+313 | VLA | | *Chandra* | 0.63 | IC/CMB | 200 | 35 | II |
| Mrk 78 | VLA | *HST* | | 0.03684 | Interaction | 3 | 3 | I |
| B2 0755+37 | MERLIN | *HST* | *Chandra* | 0.0428 | S | 4 | 4 | I |
| B2 0827+243 | X | X | X | 0.941 | | | | |
| PKS 0920−397 | X | X | *Chandra* | 0.591 | | | | |
| Q0957+561 | VLA | *HST* | *Chandra* | 1.41 | IC/CMB | 46 | 8 | |
| NGC3079 | GMRT | *HST* | *Chandra* | 0.00375 | S | 11 | 3 | |
| PKS 1030−357 | X | X | *Chandra* | 1.455 | | | | |
| PKS 1055+018 | VLA | *HST* | *Chandra* | 0.888 | | 117 | 20 | |
| PKS 1055+201 | X | X | *Chandra* | 1.11 | | | | |
| PKS 1127−145 | VLA | *HST* | *Chandra* | 1.187 | IC/CMB | 330 | 30 | I |
| PKS 1136−135 | VLA | *HST* | *Chandra* | 0.554 | S | 49 | 10 | I |
| PKS 1150+497 | VLA | *HST* | *Chandra* | 0.334 | IC/CMB | 35 | 9 | II |
| PKS 1202−262 | X | | *Chandra* | 1.95 | | | | |
| SDSS 1306+0356 | | | *Chandra* | 5.99 | IC/CMB | 158 | 23 | II |
| PKS 1354+195 | VLA | *HST* | *Chandra* | 0.72 | IC/CMB | 151 | 28 | II |
| PKS 1421−490 | ACTA | | *Chandra* | | | | | |
| PKS 1510−089 | X | X | *Chandra* | 0.361 | | | | |
| GB 1508+5714 | VLA | *HST* | *Chandra* | 4.3 | IC/CMB | 21 | 3 | II |
| B2 1553+24 | X | *HST* | *Chandra* | 0.0426 | S | 162 | 285 | I |
| B2 1658+30A | VLA | *HST* | | 0.0351 | S | 76 | 160 | I-II |
| PKS 2101−490 | X | X | *Chandra* | | | | | |
| PKS 2201+044 | VLA | *HST* | *Chandra* | 0.028 | S | 1.6 | 2 | I |
| PKS 2251+134 | VLA | *HST* | *Chandra* | 0.673 | | 21 | 3.5 | |
| 3C2 | VLA | *HST* | | 1.037 | S | 53 | 5 | II |
| 3C9 | VLA | | *Chandra* | 2.012 | IC/CMB | 57 | 10 | II |
| 3C15 | VLA | *HST* | *Chandra* | 0.073 | S | 5.1 | 4.1 | II |
| 3C19 | VLA | *HST* | | 0.482 | S | 5.5 | 1.3 | II |
| 3C20 | VLA | *HST* | | 0.174 | S | 2.4 | 1.2 | II |
| 3C31 | VLA | *HST* | *Chandra* | 0.0169 | S | 3 | 9 | I |
| 3C34 | VLA | *HST* | | 0.689 | Collision | 120 | 15 | II |
| 3C66B | VLA | *HST* | *Chandra* | 0.0215 | S | 2.9 | 7 | I |
| 3C78 | X | X | *ROSAT*/*Chandra* | 0.0288 | S | 4 | 5 | I |
| 3C98 | VLA | X | X | 0.0306 | | | | |
| 3C99 | VLA | *XMM* | | 0.426 | Collision | 3.7 | 1 | II |
| 3C120 | VLA | NOT | *Chandra* | 0.033 | S | 22 | 25 | I |
| 3C129 | VLA | X | *Chandra* | 0.0208 | S | 1.5 | 2.5 | I |
| 3C133 | VLA | *HST* | *ROSAT* | 0.2775 | S | 3.2 | 1 | II |
| 3C171 | VLA | *HST* | *ROSAT* | 0.2384 | S | 3.9 | 1.4 | II |
| 3C179 | VLA | *HST* | *Chandra* | 0.846 | IC/CMB | 39 | 7 | II |

Table 5: Quasar jets (continued)

| | | | | | | | | |
|---|---|---|---|---|---|---|---|---|
| 3C179 | VLA | *HST* | *Chandra* | 0.846 | IC/CMB | 39 | 7 | II |
| 3C196.1 | VLA | *HST* | | 0.198 | S | 3 | 1.3 | II |
| 3C200 | X | *HST* | *Chandra* | 0.458 | S | 10 | 2.5 | II |
| 3C207 | VLA | X | *Chandra* | 0.684 | IC/CMB | 48 | 6 | II |
| 3C212 | X | *HST* | *Chandra* | 1.049 | S | 107 | 10 | II |
| 3C219 | VLA | X | *Chandra* | 0.1744 | IC/IR | 80 | 40 | II |
| 3C223 | VLA | X | *XMM* | 0.136928 | | 187 | 120 | II |
| 3C245 | VLA | *HST* | *ROSAT* | 1.029 | S | 84 | 8 | II |
| 3C264 | MERLIN | *HST* | *Chandra* | 0.0208 | S | 0.27 | 0.72 | I |
| 3C265 | VLA | *HST* | *Chandra* | 0.811 | Collision | 248 | 30 | II |
| 3C268.3 | VLA | *HST* | *ROSAT* | 0.371 | S | 5.6 | 1.3 | II |
| 3C270 | VLA | *HST* | *Chandra* | 0.0074 | S or IC/Q | 0.4 | 24 | I |
| 3C273 | VLA | *HST* | *Chandra* | 0.158 | IC/CMB | 27 | 15 | II |
| 3C277.2 | VLA | X | *ROSAT* | 0.766 | IC/(CMB+Q) | 154 | 20 | II |
| 3C279 | VLA | *HST* | *Chandra* | 0.536 | S | 3.3 | 0.6 | |
| 3C284 | VLA | X | *XMM* | 0.2394 | | 480 | 174 | II |
| 3C293 | MERLIN | *HST* | | 0.045034 | S | 120 | 119 | |
| 3C292 | VLA | X | *XMM* | 0.71 | IC/CMB | 261 | 36 | II |
| 3C295 | VLA | *HST* | *Chandra* | 0.461 | SSC | 11 | 1.9 | II |
| 3C296 | VLA | *HST* | | 0.025814 | Collision | | | |
| 3C303 | VLA | NOT | *Chandra* | 0.141 | SSC+IC/(CMB) | 36 | 17 | II |
| 3C322 | VLA | | *XMM* | 1.68 | SSC+IC/(CMB) | 103 | 15 | II |
| 3C334 | VLA | X | *ROSAT* | 0.555 | | 112 | 16 | II |
| 3C346 | X | *HST* | *Chandra* | 0.161 | S | 2.6 | 1.4 | II |
| 3C356 | VLA | *HST* | *ROSAT* | 1.086 | IC/(CMB+Q) | 256 | 36 | II |
| 3C371 | VLA | *HST* | *Chandra* | 0.051 | Collision-S | 3.6 | 4 | II |
| 3C390.3 | VLA | MMT | *ROSAT*/*Chandra* | 0.057 | Collision-S | 117 | 105 | II |
| 3C410 | VLA | *HST* | | 0.2485 | S | 2.9 | 1 | II |
| 3C449 | VLA | *HST* | *XMM* | 0.0215 | Interaction | 209 | 600 | I |
| 3C459 | VLA | *HST* | | 0.22 | Collision | 11.6 | 4.5 | II |
| 4C41.17 | VLA | | *Chandra* | 3.8 | IC/Q | 100 | 15 | II |
| ESO 295−IG022 | ATCA | X | *ROSAT* | 0.054824 | IGM interaction | 96 | 90 | |
| Cen A | VLA | *HST* | *Chandra* | 0.007 | S | 4 | 240 | I |
| Cen B | ATCA | X | *ASCA* | 0.01215 | IC/CMB | 14 | 472 | I |
| Coma A | X | *HST* | | 0.0857 | Collision | 96 | 45 | I-II |
| Cyg A | VLA | IR | *Chandra* | 0.0562 | SSC | 76 | 62 | I |
| Fornax A | VLA | X | *Chandra* | 0.005871 | IC/CMB | 96 | 900 | II |
| NGC315 | X | X | *ROSAT* | 0.016485 | | 64 | 240 | I |
| M84 (3C373.1) | VLA | *HST* | *Chandra* | 0.0037 | S | 0.32 | 3.9 | I |
| M87 (3C274) | VLA | *HST* | *Chandra* | 0.0043 | S | 2.3 | 30 | I |
| Pic A | VLA | *HST* | *Chandra* | 0.0342 | IC/CMB | 240 | 252 | II |
| NGC6217 | VLA | *HST* | *ROSAT* | 0.00533 | SSC | 18.8 | 160 | II |
| NGC6251 | X | *HST* | *Chandra* | 0.024881 | | 97 | 240 | I/II |

Table 6: Quasar jets (spectral indices)

| Object | $\alpha(r)$ | $\alpha(r-o)$ | $\alpha(o-x)$ | $\alpha(x)$ | RA 2000.0 | Dec 2000.0 |
|---|---|---|---|---|---|---|
| NGC315 | | | | 1.5 | 00h 57m 48.8s | 30° 21′ 09″ |
| B2 0206+35 | | | | 1.05 | 02h 09m 38.6s | 35° 47′ 50″ |
| B2 0326+39 | | | | | 03h 29m 24.2s | 39° 47′ 42″ |
| PKS 0521−365 | | 0.76 | | | 05h 22m 58.0s | −36° 27′ 31″ |
| PKS 0606−085 | | | | | 06h 07m 59.7s | −08° 34′ 49″ |
| PKS 0637−752 | 0.81 | | | 0.85 | 06h 35m 48s | −75° 16′ 00″ |
| B2 0738+313 | 0.9 | | | 1.01 | 07h 41m 10.7s | 31° 12′ 00″ |
| Mrk 78 | | | | | 07h 42m 41.7s | 65° 10′ 37″ |
| B2 0755+37 | | | | | 07h 58m 28.2s | 37° 47′ 12″ |
| B2 0827+243 | | | | | 08h 30m 52.1s | 24° 11′ 00″ |
| PKS 0920−397 | | | | | 09h 22m 46.4s | −39° 59′ 35″ |
| Q0957+561 | | | | 0.87 | 10h 01m 21s | 55° 53′ 57″ |
| NGC3079 | 1.01 | | | | 10h 01m 57.8s | 55° 40′ 47″ |
| PKS 1030−357 | | | | | 10h 33m 07.7s | −36° 01′ 57″ |
| PKS 1055+018 | | >2.27 | | | 10h 58m 29.6s | 01° 33′ 59″ |
| PKS 1055+201 | | | | | 10h 58m 17.9s | 19° 51′ 51″ |
| PKS 1127−145 | 0.84 | | | 0.5 | 11h 30m 07.1s | −14° 49′ 27″ |
| PKS 1136−135 | | 0.89 | 0.76 | | 11h 39m 10.6s | −13° 50′ 44″ |
| PKS 1150+497 | | 1.14 | 0.66 | | 11h 53m 24.5s | 49° 31′ 09″ |
| PKS 1202−262 | | | | | 12h 02m 01.9s | −26° 07′ 41″ |
| SDSS 1306+0356 | | | 1.65 | | 13h 06m 08.2s | 03° 56′ 26″ |
| PKS 1354+195 | | 1.1 | 0.64 | | 13h 57m 06s | 19° 19′ 00″ |
| PKS 1421−490 | | | | | 14h 24m 30s | −49° 14′ 00″ |
| PKS 1510−089 | | | | | 15h 12m 50.6s | −09° 06′ 00″ |
| GB 1508+5714 | | | | 0.91 | 15h 10m 02.9s | 57° 02′ 43″ |
| B2 1553+24 | | | | | | |
| B2 1658+30A | | | | | 17h 00m 45.2s | 30° 08′ 09″ |
| PKS 2101−490 | | | | | 21h 05m 01.2s | −48° 48′ 47″ |
| PKS 2201+044 | | 0.85 | | | 22h 04m 17.6s | 04° 40′ 02″ |
| PKS 2251+134 | | >1.89 | | | 22h 54m 21.0s | 13° 41′ 48″ |
| 3C2 | | 0.73 | | | 00h 06m 22.6s | −00° 04′ 25″ |
| 3C9 | 1 | | | 0.6 | 00h 20m 25s | 15° 40′ 53″ |
| 3C15 | | 0.95 | | | 00h 37m 04s | −01° 09′ 08″ |
| 3C19 | 0.6 | | | | 00h 40m 55s | 30° 10′ 08″ |
| 3C20 | 0.67 | | | | 00h 43m 08.8s | 52° 03′ 34″ |
| 3C31 | 0.57 | | | | 01h 07m 25s | 32° 24′ 45″ |
| 3C34 | 1 | | | | 01h 10m 18.7s | 31° 47′ 20″ |
| 3C66B | | | | | 02h 23m 11.4s | 42° 59′ 31″ |
| 3C78 | 0.43 | | | | 03h 08m 26.2s | 04° 06′ 39″ |
| 3C98 | | | | | 03h 58m 54.4s | 10° 26′ 03″ |
| 3C99 | 0.82 | | | | 04h 01m 07.6s | 00° 36′ 33″ |
| 3C120 | 0.65 | 0.8 | | | 04h 33m 11.1s | 05° 21′ 16″ |
| 3C129 | 0.8 | | 0.9 | 0.9 | 04h 49m 09.1s | 45° 00′ 39″ |
| 3C133 | 0.7 | | | | 05h 02m 58.6s | 25° 16′ 25″ |
| 3C171 | 0.87 | | | | 06h 55m 14.8s | 54° 09′ 00″ |
| 3C179 | | >0.91 | <0.73 | | 07h 28m 11.7s | 67° 48′ 48″ |

Table 7: Quasar jets (spectral indices continued)

| Object | $\alpha(r)$ | $\alpha(r-o)$ | $\alpha(o-x)$ | $\alpha(x)$ | RA 2000.0 | Dec 2000.0 |
|---|---|---|---|---|---|---|
| 3C196.1 | 1.16 | | | | 08h 15m 27.8s | $-03°\ 08'\ 27''$ |
| 3C200 | 0.84 | | | | 08h 27m 25.4s | $29°\ 18'\ 45''$ |
| 3C207 | 0.9 | | | 0.4 | 08h 40m 47.5s | $13°\ 12'\ 23''$ |
| 3C212 | 0.83 | | 1.39 | | 08h 58m 41.5s | $14°\ 09'\ 44''$ |
| 3C219 | 0.65 | | | 0.74 | 09h 21m 08.6s | $45°\ 38'\ 57''$ |
| 3C223 | | | | | 09h 39m 52.7s | $35°\ 53'\ 58''$ |
| 3C245 | 0.72 | | 0.41 | | 10h 42m 44.6s | $12°\ 03'\ 31''$ |
| 3C264 | | 0.58 | | | 11h 45m 05.0s | $19°\ 36'\ 23''$ |
| 3C265 | | | | | 11h 45m 29.0s | $31°\ 33'\ 49''$ |
| 3C268.3 | 0.5 | | | | 12h 06m 24.7s | $64°\ 13'\ 37''$ |
| 3C270 | | 0.85 | | 0.3 | 12h 19m 23.2s | $05°\ 49'\ 31''$ |
| 3C273 | | | | | 12h 29m 06.7s | $02°\ 03'\ 09''$ |
| 3C277.2 | 0.95 | | | 0.95 | 12h 53m 33s | $15°\ 42'\ 29''$ |
| 3C279 | 0.79 | $>1.1$ | 1.6 | | 12h 56m 11.2s | $-05°\ 47'\ 22''$ |
| 3C284 | | | | | 13h 11m 04.7s | $27°\ 28'\ 08''$ |
| 3C293 | | | | | 13h 52m 17.8s | $31°\ 26'\ 47''$ |
| 3C292 | | | | 0.88 | 13h 50m 41.9s | $64°\ 29'\ 31''$ |
| 3C295 | 0.7 | 1.5 | | | 14h 11m 20.6s | $52°\ 12'\ 09''$ |
| 3C296 | | | | | 14h 16m 52.7s | $10°\ 48'\ 11''$ |
| 3C303 | | | | 1 | 14h 43m 02.8s | $52°\ 01'\ 37''$ |
| 3C322 | | | | 0.6 | 15h 35m 01.2s | $55°\ 36'\ 53''$ |
| 3C334 | | | | | 16h 20m 21.9s | $17°\ 36'\ 24''$ |
| 3C346 | 0.54 | | | | 16h 43m 48.7s | $17°\ 15'\ 49''$ |
| 3C356 | | | | | 17h 24m 19s | $50°\ 57'\ 40''$ |
| 3C371 | 0.72 | 0.81 | | | 18h 06m 50.7s | $69°\ 49'\ 28''$ |
| 3C390.3 | 0.7 | | 0.95 | 0.95 | 18h 42m 09.0s | $79°\ 46'\ 17''$ |
| 3C410 | 0.56 | 0.9 | | | 20h 20m 06.6s | $29°\ 42'\ 14''$ |
| 3C449 | 1 | | | | 22h 31m 20.9s | $39°\ 21'\ 48''$ |
| 3C459 | | | | | 23h 16m 35.2s | $04°\ 05'\ 18''$ |
| 4C41.17 | | | | 0.57 | 06h 50m 52.1s | $41°\ 30'\ 31''$ |
| ESO 295−IG022 | | | | | 00h 55m 45.9s | $-37°\ 24'\ 28''$ |
| Cen A | | | | 1 | 13h 25m 27.6s | $-43°\ 01'\ 09''$ |
| Cen B | 0.78 | | | 0.88 | 13h 46m 48.3s | $-60°\ 24'\ 34''$ |
| Coma A | | | | | 12h 54m 11.7s | $27°\ 37'\ 33''$ |
| Cyg A | 0.55 | 1.02 | | 0.8 | 19h 59m 28.4s | $40°\ 44'\ 02''$ |
| Fornax A | | | | | 03h 22m 41.7s | $-37°\ 12'\ 30''$ |
| NGC315 | | | | | 00h 57m 48.9s | $30°\ 21'\ 09''$ |
| M84 (3C373.1) | 0.65 | 0.86 | | 0.8 | 12h 25m 03.8s | $12°\ 53'\ 13''$ |
| M87 (3C274) | | | | | 12h 30m 49.4s | $12°\ 23'\ 28''$ |
| Pic A | 0.8 | | | 0.6 | 05h 19m 49.7s | $-45°\ 46'\ 45''$ |
| NGC6217 | | | | 0.6 | 16h 32m 39.2s | $78°\ 11'\ 53''$ |
| NGC6251 | | | | | 16h 32m 32.0s | $82°\ 32'\ 16''$ |